Journal of Genetic Engineering and Biotechnology 23 (2025) 100470

Contents lists available at ScienceDirect

Journal of Genetic Engineering and Biotechnology

journal homepage: www.elsevier.com/locate/jgeb

NanoFlora: Unveiling the therapeutic potential of *Ipomoea aquatica* nanoparticles

Manickavasagam Sasikala [a,b,*], Sellappan Mohan [a,b,*], Arjunan Karuppaiah [a,b,c], Vedi Karthick [a,b], Palanigoundar Atheyannan Ragul [a,b], Arumugam Nagarajan [a,b]

[a] *Karpagam College of Pharmacy, Coimbatore 641 032 Tamil Nadu, India*
[b] *The Tamil Nadu Dr. M.G.R. Medical University, Chennai 600032 Tamil Nadu, India*
[c] *PSG College of Pharmacy, Peelamedu, Avinashi Road, Coimbatore 641004, India*

ARTICLE INFO

Keywords:
Antioxidant
Antidiabetic
DPPH
Ipomoea aquatica
HPTLC
Metal nano particles
Silver nanoparticles
Bioautographic method

ABSTRACT

Introduction: Improving the pharmacokinetics of drugs is achieved through nano formulations and the role of natural product in the synthesis of nanomaterials is gaining prominence due to its eco-friendly nature, cost-effectiveness, and demonstrated efficacy. Metal nanoparticles (NPs) derived from *Ipomoea aquatica* Forsskal have been synthesized and evaluated for their antioxidant and antidiabetic properties towards enhancing the anticancer activity of the plant extracts.

Methodology: Hydroalcoholic extract was obtained from the entire Ipomoea aquatica plant and utilized as a key ingredient in the green synthesis of metal NPs. The characterization of the synthesized NPs involved UV/visible and FT-IR spectroscopic analyses, along with particle size determination using Zetasizer technology. Antioxidant activity was assessed through DPPH radical scavenging assays, while antidiabetic potential was evaluated via alpha-amylase inhibitory activity using HPTLC bioautography.

Results: The formation of silver nanoparticles (AgNPs) was confirmed by a color change from light brown to dark brown. UV–VIS spectrum analysis showed strong absorbance between 380 and 400 nm, with a peak at 428 nm, indicating successful synthesis via bioreduction by *Ipomoea aquatica* extract. FT-IR spectra revealed phytochemicals like flavonoids and proteins, with shifts in peak positions confirming AgNP formation. DLS showed an average particle size of 36.27 nm, and TEM images confirmed spherical morphology. The AgNPs exhibited significant antioxidant and antidiabetic activities, outperforming standards such as ascorbic acid and Glibenclamide. Toxicity prediction identified the extract as slightly toxic, guiding safe dose administration.

Conclusion: The study underscores the potential of plant-based nanoparticles in scavenging free radicals and supporting cytotoxicity, thus hinting at their potential role in cancer therapy. Moreover, the nanoparticles derived from Ipomoea aquatica exhibit promising antioxidant and antidiabetic activities compared to the crude plant extract. This research paves the way for further exploration of *Ipomoea aquatica* nanoparticles as a novel therapeutic intervention for various diseases.

1. Introduction

Nanoparticles (NPs) are colloidal solid particles with dimensions in the range of 1–1000 nm. In the arena of nanomedicine, NPs are most commonly discussed as particles ranging from 5 to 100 nm that are favorable for the diagnosis and management of various diseases and systemic obstacles.[1] Nanoparticles (NPs) are widely acknowledged for their diverse advantages in biomedical applications, attributed to their unique physicochemical properties. They exhibit distinct characteristics in biological, magnetic, optical, and electronic domains at cellular, nuclear, and molecular levels, owing to their high surface-to-volume ratio. Furthermore, the surface of NPs provides an opportunity for the incorporation of various active complexes, enhancing their targeting efficiency and specificity.[2–3] Green synthesized NPs could be used to improve antioxidant and antidiabetic activity. Silver (Ag^{+}) is described as a multi-functional medicinal product in the past century, and silver nanoparticles (AgNPs) have antimicrobial, antiviral, and anticancer activity.[4,6] AgNPs possess an ease of incorporation of a number of active

* Corresponding authors at: Department of Pharmaceutical Analysis, Karpagam College of Pharmacy, Coimbatore 641 032, Tamil Nadu, India.
E-mail addresses: sasikala@kcp.edu.in (M. Sasikala), selvaamohan@gmail.com (S. Mohan), nagarajan.a@kcp.edu.in (A. Nagarajan).

https://doi.org/10.1016/j.jgeb.2025.100470
Received 14 March 2024; Received in revised form 2 January 2025; Accepted 6 February 2025

compounds on the surface and have improved pharmacological activities with reduced toxicity,[5] which gives them great importance due to their wide variety of applications in cancer targeting.[6–7] The NPs approach is constructed to target reactive oxygen species easily in order to reduce the generation of chronic diseases.[8–9] AgNPs grafted with drug conjugate could release the drug from the surface of AgNPs due to the acidification of the intracellular environment by oxidative stress generated by mitochondria.[10–11] Ipomoea aquatica is naturally grown in river and small water bands and ought to be reported to possess a number of pharmacological effects, including antioxidant, anticancer, antimicrobial, and anti-inflammatory activity. In the Unani system of medicine, Ipomoea aquatica is used in the treatment of piles and fever.[12–13] The novelty of this study lies in the development of a novel and sensitive dose-densitometric bioautographic high-performance thin-layer chromatography (HPTLC) method for the analysis of IA-AgNPs, which has not been previously reported.

The purpose of this research is to produce Ipomoea aquatica-mediated AgNPs (IA-AgNPs) ensuing the green synthesis method and to assess the cost-effective bioautographic antioxidant and antidiabetic activities of AgNPs exposed to free radical scavenging of DPPH and starch-iodine complex methods when compared to the existing invitro cell viability methods.

2. Material and methods

2.1. Materials

Silver nitrate, ethanol, methanol, ethyl acetate, n-hexane, acetic acid, anisaldehyde, 2,2-diphenyl-1-picrylhydrazyl (DPPH), and ascorbic acid were obtained from S D Fine Chemicals Limited, Mumbai. HPTLC-pre-coated silica gel 60 F254 aluminum plates (20x10 cm) were procured from Merck Specialties Private Limited, Mumbai (400 018). 2,2-Di (4-*tert*-octylphenyl)-1-picrylhydrazyl (DPPH) free radical, iron(III) chloride (97 %), gallic acid (97 %), α-amylase, Bacillus licheniformis liquid, and β-glucosidase were purchased from Sigma-Aldrich, Bangalore, India, and BDH, Poole, England. All substances used were of analytical reagent (AR) grade.

2.1.1. α-amylase inhibitory activity

To prepare a 1 % (w/v) α-amylase solution, almost 1.25 mL (1 g based on the density and concentration of the commercially available stock solution) of α-amylase obtained from *Bacillus licheniformis* liquid was diluted with distilled water to a final volume of 100 mL. This enzyme stock solution was then stored at 4 °C until required. The plates were treated with the α-amylase solution and located in a flexible flask with plugs to confirm consistency. The vessel was filled with water to preserve moistness during a 30-minute incubation period at 37 °C, allowing for the main reaction among the enzymes and inhibitors existing in the extracts. Following incubation, the plates were immersed in a 1 % starch solution for 10–20 min to facilitate the enzyme-substrate reaction. Subsequently, they were splashed with Gram's iodine solution, which served as the detection solution,[14,33] before capturing an image of the plate.

2.2. Preparation of Ipomoea aquatica extracts (IAE)

The *Ipomoea aquatica* (IA) plants were collected and washed thoroughly with distilled water three times. Following the washing, the plants were dried under sunlight and then finely ground into a powder. This powder underwent hydroalcoholic extraction using a cold percolation method with a mixture of water and 95 % ethanol (1:1 v/v). The resulting extract was concentrated using a rotary evaporator to obtain a concentrated extract. Analysis of the aqueous alcoholic extract of the whole plant of *I. aquatica* revealed the presence of various compounds, including flavonoids, saponins, tannins, alkaloids, glycosides, phenols, terpenoids, and coumarins (Table 1). Further analysis of the leaves of *I. aquatica* identified triterpenes, flavonoids, saponins, alkaloids, tannins, glycosides, and additional flavonoids. Additionally, a qualitative assessment of total phenols in the methanol extract of *I. aquatica* showed a concentration of 0.83 ± 0.06 mg GAE/g extract.

Table 1
Presence of phytochemicals in Hydroalcoholic of *I. Aquatica.*

S. No.	Metabolites	Phyto-constituents	Inference
	Primary metabolites	Carbohydrates	+ (Reducing sugar, Ketoses, Pentoses, Glucose and Mannose)
		Proteins	+
		Amino acids	+
	Secondary metabolites	Alkaloids	+
		Glycosides	+
		Flavonoids	+
		Tannins	+ (hydrolysable tannins)
		Steroids and TriterpenoidsTest	+ (Tri-terpenoids)

Note: '+' indicates the presence of the test.

2.3. Synthesis of IA-AgNPs

The concentration of the vegetal extract used for the synthesis of nanoparticles was 2 mg/mL. Upon the addition of 5 mM $AgNO_3$, the color of the extract rapidly changed to brown within 30 min, with no further observable alteration after 24 h (Fig. 1). The observed color change can be attributed to the presence of active phytochemicals within the *I. aquatica* extract. These phytochemicals act as reducing agents, facilitating the transformation of silver ions into AgNPs through the excitation of surface plasmon resonance. The bioreduction of Ag^+ ions from the $AgNO_3$ solution into silver nanoparticles using phytochemicals from *I. aquatica* was confirmed through UV–Visible spectroscopy.

AgNPs were synthesized by slowly adding 50 mL of IA extract dropwise into 50 mL of a freshly prepared aqueous silver nitrate (AgNO3) solution with a concentration of 1 mM in a glass beaker. The mixture was stirred continuously using a magnetic stirrer at room temperature (24 °C). After suspension, the solution underwent centrifugation at 1500 rpm for 1 h. The resulting solid particles were collected and subsequently dried in a beaker on a hot plate at 80 °C for 2 h. Following this, the dried powder was finely ground using a mortar and pestle to achieve the desired AgNPs. These AgNPs were then transferred into an Eppendorf tube and stored in a refrigerator for further analysis.

2.4. Characterization of green synthesized IA-AgNPs

2.4.1. UV–VIS spectrophotometric analysis

The primary formation of nanoparticles (NPs) was identified using a double-beam UV–VIS spectrophotometer (UV-1800, Shimadzu). The sample was diluted with deionized water and placed into a quartz cell for recording the absorbance spectrum across the wavelength range from 200 to 800 nm, with deionized water serving as the blank reference. The band gap of the AgNPs was determined using the standard formula. Eg 398 nm is the energy band gap (eV) and is the maximum wavelength of the absorption band (nm).

2.4.2. Fourier transform infrared (FT-IR) analysis

FT-IR spectroscopy was employed to ascertain the functional groups present on the surface of AgNPs by observing the stretching and bending frequencies of the molecules. The functional groups of NPs were examined within the range of 400 to 4000 cm1 using a NicoletTM iSTM ™ 5 FTIR spectrometer.

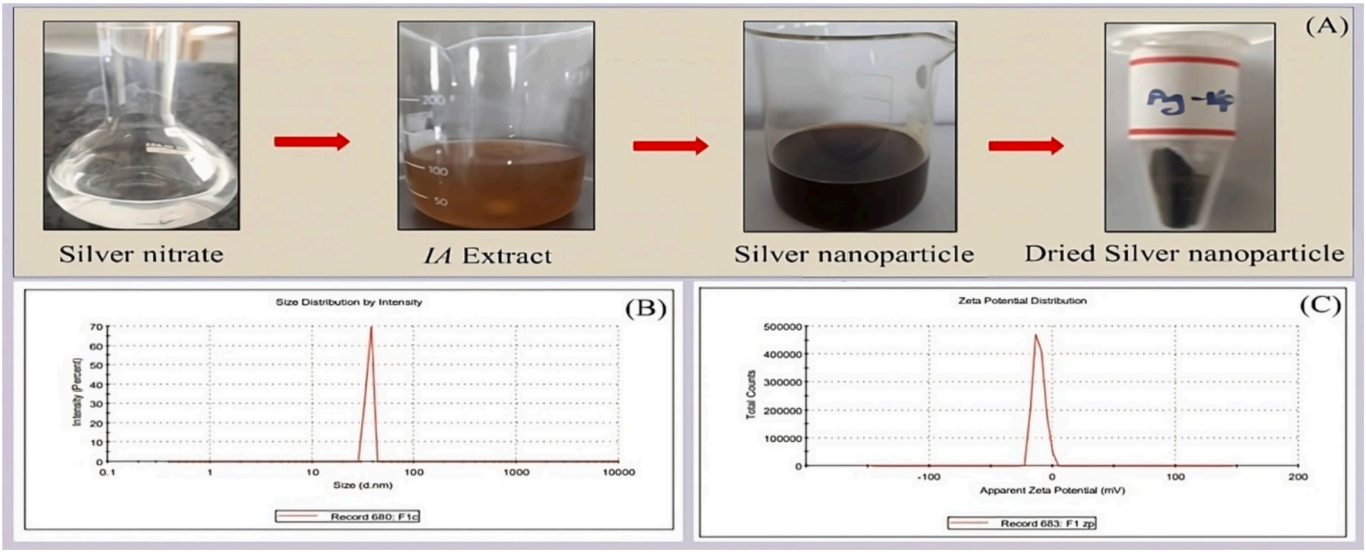

Fig. 1. Green synthesis of silver nanoparticles from *Ipomoea aquatica* (IA-AgNPs). (For interpretation of the references to color in this figure legend, the reader is referred to the web version of this article.)

2.4.3. Transmission electron microscopy (TEM)

Morphological analysis of the AgNPs was conducted using Transmission Electron Microscopy (TEM 120 kV; T12 Fei, Tecnai G2 Spirit TWIN).

2.4.4. Energy dispersive analysis of X-rays (EDAX)

XRD analysis was performed to determine the crystalline nature of the synthesized nanoparticles. The diffractogram showed characteristic peaks, corresponding to the face-centered cubic structure of silver nanoparticles. Observations on the elemental composition of the AgNPs were carried out using Energy Dispersive Analysis of X-rays (EDAX) on a JEOL JEM-2100.

2.4.5. Antioxidant and α-amylase activity of IA-AgNPs

To evaluate antioxidant activity, a high-performance thin-layer chromatographic (HPTLC) bioautographic method was employed to assess DPPH scavenging activity. The assay was conducted on normal-phase Silica Gel 60 F254 Aluminum Plates using a mobile phase composed of n-hexane, ethyl acetate, and acetic acid (20:9:1). IA-AgNPs were sprayed onto the plates, and calibration was carried out using standard solutions of ascorbic acid, glibenclamide, and acarbose. Following plate development, they were immersed in a DPPH solution and stored in darkness before scanning. Subsequently, the plates underwent derivatization with anisaldehyde-sulfuric acid, heating, and scanning.

To evaluate the ability of the IA-AgNPs to inhibit α-amylase activity, a single-step gradient elution utilizing n-hexane, ethyl acetate, and acetic acid (20:9:1) was employed over an 80-mm developing distance. The plates were immersed in a α-amylase solution (1 % w/v) for the primary reaction, allowing 10–20 min, followed by dipping in a starch solution (1 % w/v potato starch) for another 10–20 min to facilitate the secondary reaction. Finally, the plates were washed with Gram's iodine solution for detection.

2.5. Toxicity prediction

The drug likeness and toxicity prediction were evaluated using ProTox-II, specialized software designed for predicting chemical toxicity. ProTox-II employs a variety of methodologies, including molecular similarity, fragment propensities, most frequent features, and machine learning based on fragment similarity. It integrates a total of 33 models to predict various toxicity endpoints, such as acute toxicity, hepatotoxicity, cytotoxicity, carcinogenicity, mutagenicity, immunotoxicity, adverse outcomes pathways (Tox21), and toxicity targets. Toxicity classes are classified according to the globally harmonized system of classification and labeling of chemicals (GHS), with LD50 values provided in mg/kg. These toxicity classes are defined as follows: Class I: fatal if swallowed (LD50 $\leq$ 5); Class II: fatal if swallowed (5 $<$ LD50 $\leq$ 50); Class III: toxic if swallowed (50 $<$ LD50 $\leq$ 300); Class IV: harmful if swallowed (300 $<$ LD50 $\leq$ 2000); Class V: may be harmful if swallowed (2000 $<$ LD50 $\leq$ 5000); Class VI: non-toxic (LD50 $>$ 5000).[15]

3. Result and Discussion

The formation of silver nanoparticles was confirmed by observing a color change from light brown to dark brown (Fig. 1A). Additionally, a visual inspection revealed a transition from brownish yellow to dark brown, further indicating the formation of AgNPs. To confirm nanoparticle formation, the UV–VIS spectrum of the colored suspension was recorded. The colloidal solution exhibited strong absorbance in the range of 350–450 nm (Fig. 2), with AgNPs displaying a band gap value of approximately 3.22 eV.[16] Notably, the highest absorbance peak was observed at 398 nm, accompanied by the appearance of a symmetric peak for *I. aquatica* (Fig. 2), which signifies the formation of AgNPs through the bioreduction of silver by the active compounds present in *Ipomoea aquatica* extract.

The FT-IR spectra of the extract and synthesized IA-AgNPs are depicted in Fig. 3. Phytochemical analysis of IA indicates the presence of flavonoids, alkaloids, steroids, saponins, and proteins. In the IA extract, peaks were observed at 3292 cm^{-1}, 1592 cm^{-1}, 1381 cm^{-1}, 1259 cm^{-1}, and 1046 cm^{-1}. Conversely, in the IA-AgNPs, peaks were observed at 3297 cm^{-1}, 1595 cm^{-1}, 1374 cm^{-1}, 1258 cm^{-1}, and 1070 cm^{-1} (Fig. 3). The peak at 3292 cm^{-1} corresponds to O–H stretching vibrations, while the vibration stretch at 1592 cm^{-1} indicates C=C stretch in the aromatic ring, confirming the presence of aromatic groups. The C-O stretching vibrations of the IR spectrum are observed at 1046 cm^{-1}. Notably, in the IA-AgNPs, peak positions shifted slightly from 3292 cm^{-1} to 3297 cm^{-1}, 1592 cm^{-1} to 1595 cm^{-1}, 1381 cm^{-1} to 1374 cm^{-1}, 1259 cm^{-1} to 1258 cm^{-1}, and 1046 cm^{-1} to 1070 cm^{-1}. It is known that IA extract possesses biological activity due to the presence of phenolic, aldehyde, and ether linkages, which may contribute to the biological reduction of Ag + to Ag0[17–19].

Dynamic Light Scattering (DLS) is utilized to ascertain the size and size distribution profile of particles in a colloidal suspension

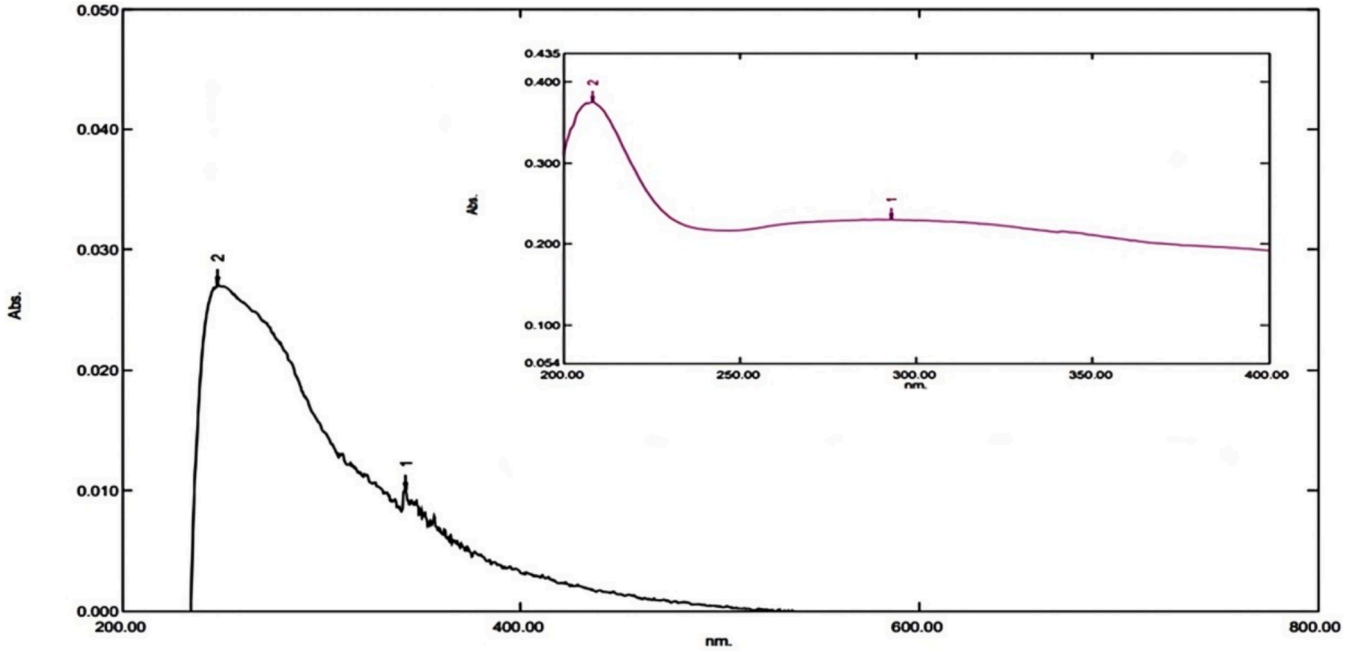

Fig. 2. UV–Vis spectra of (a) hydroalcoholic extract of Ipomoea aquatica and (b) silver nanoparticles synthesized using the extract, showing surface plasmon resonance (SPR) at 410 nm.

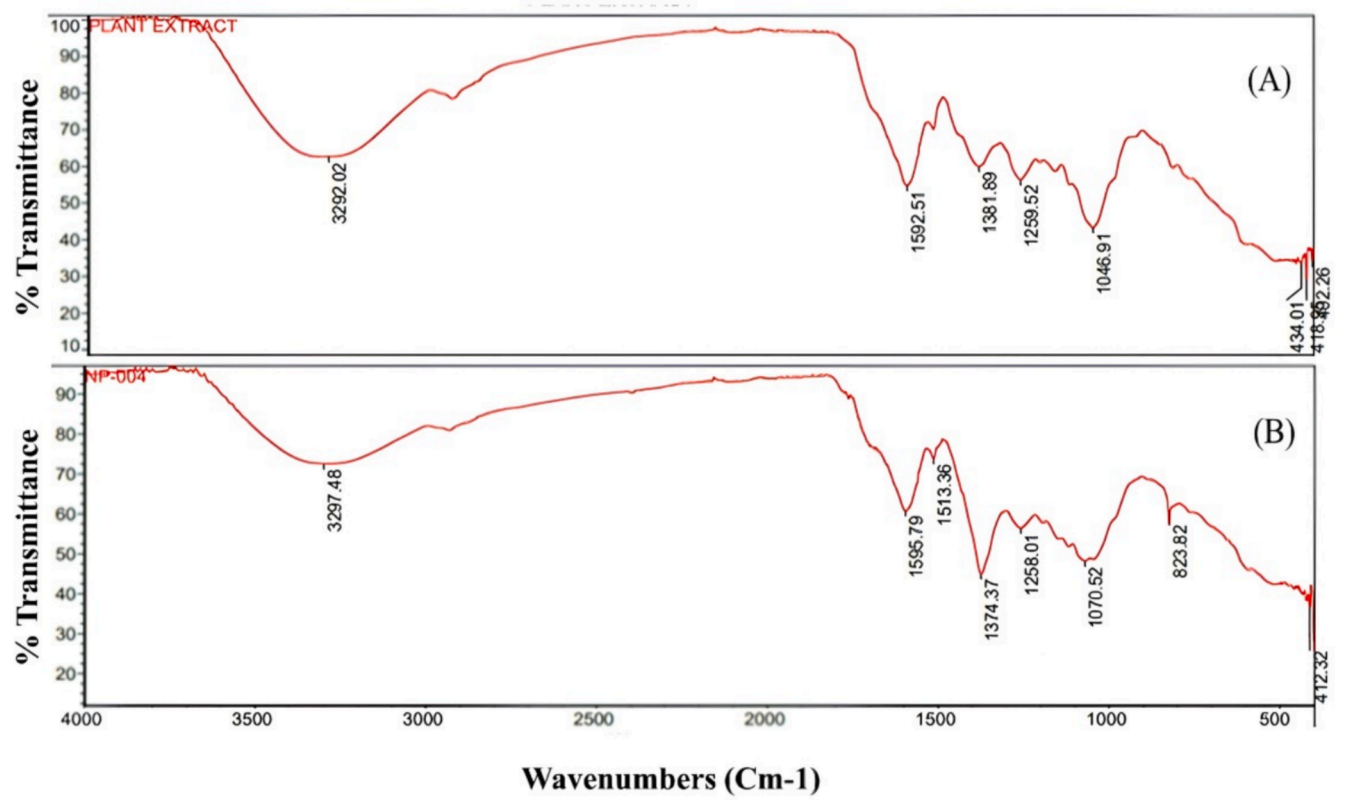

Fig. 3. FTIR spectrum of IA-AgNPs.

(Fig. 1B&C). The DLS graph of IA-AgNPs revealed an average size of 36.27 nm, with the particles carrying a charge of −11 mV. Zeta potential measurement assesses the potential stability of particles in the colloidal suspension, where AgNPs generally exhibit a negative charge. Synthesized IA-AgNPs exhibited a negative charge and remained stable at room temperature.[20–21]

TEM micrographs of AgNPs depicted spherical morphology, with particles being monodispersed and sized less than 100 nm (Fig. 4A), as evidenced by the appearance of bright-field TEM images. These results indicate that Ipomoea aquatica mediated the formation of spherical and uniform AgNPs. The extract functions as a reducing agent in the preparation of AgNPs due to its antioxidant properties.

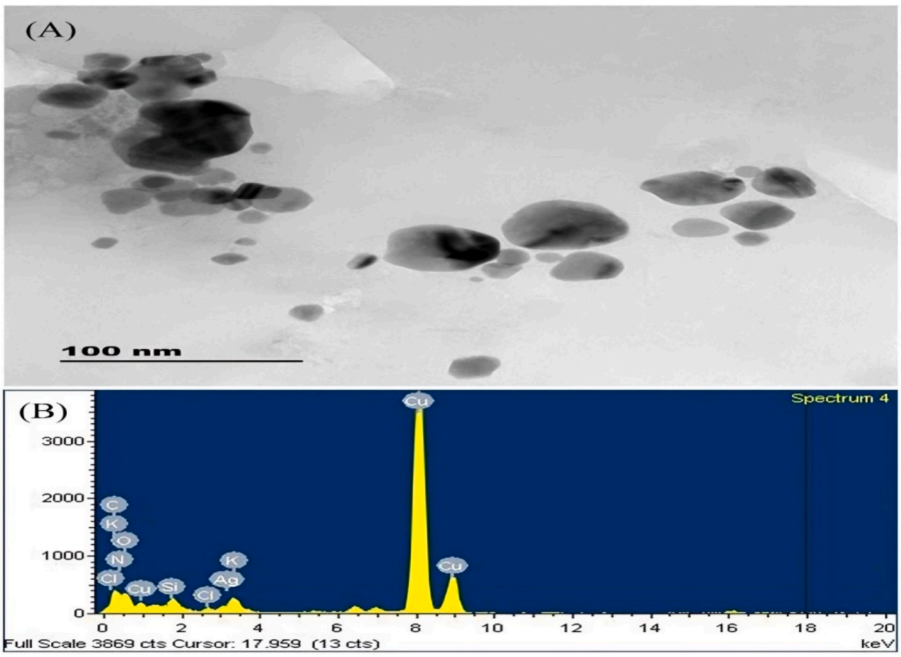

Fig. 4. TEM (A) and EDAX (B) spectra of IA-AgNPs.

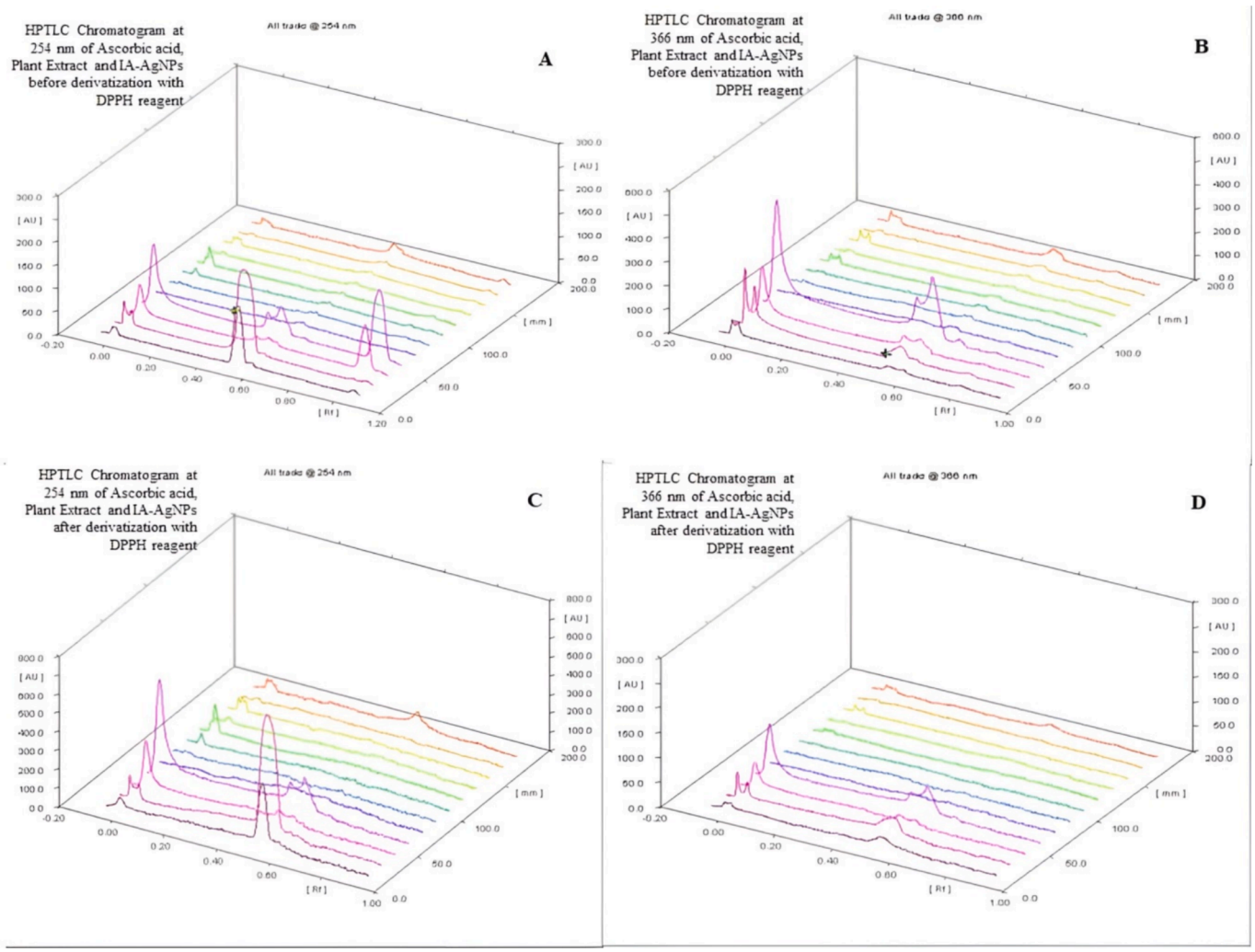

Fig. 5. (HPTLC-DPPH assay) DPPH scavenging activities of IA extract, IA-AgNPs and Standard Ascorbic acid.

Furthermore, the spherical morphology and size of NPs less than 100 nm, as determined by chemical analysis using EDS after 1 h of reaction time, support the notion that Ipomoea aquatica extract can act as a reducing agent in AgNP preparation. This green synthesis process of AgNPs occurs due to the antioxidant properties of *Ipomoea aquatica* extract.

The EDAX pattern indicates the presence of silver as the key constituent metal in the synthesized nanoparticles, as observed through energy-dispersive spectrum analysis. Metallic silver nanoparticles exhibit a specific intense peak around 3 keV, attributed to surface plasmon resonance. The figure depicts the presence of elements such as C, N, O, Na, and Ag in the biochemically synthesized AgNPs mediated by *Ipomoea aquatica* (Fig. 4B). The strong absorption in the range of 3–3.5 keV confirms the formation of AgNPs.

DPPH scavenging activity was measured for the IP extract [second four tracks from the chromatogram], IA-AgNP's [third four tracks from the chromatogram], and standard ascorbic acid [first four tracks from the chromatogram], yielding values of 45.15, 96.05, and 90.73, respectively (Fig. 5A,B,C&D). Remarkably, the AgNP's exhibited enhanced reducing power compared to ascorbic acid, likely attributed to the nanostructure of the AgNPs. It is worth noting that free radicals and H_2O_2 may influence the disintegration of AgNPs, leading to the accumulation of hydroxyl radicals and subsequent elevation of oxidative stress, as reported by Yang et al.,[22] who described the role of AgNPs in causing inflammatory responses. Our findings also indicate that the IA extract and its silver nanoparticles can protect against oxidative DNA damage, similar to the report by Xingping and Sugapriya.[23]

Polyphenols like eugenol and pyrogallol extracted from cinnamon have displayed promising antidiabetic properties along with the ability to stimulate the rejuvenation of beta cells.[24] Similarly, polysaccharides found in mulberry leaf have shown enhanced insulin secretion and the capacity to inhibit α-glucosidase activity, contributing to diabetes management.[25–26] The significance of reducing reactive oxygen species (ROS) levels in managing diabetes-related complications has been underscored.[27–29] High levels of ROS exacerbate pancreatic beta-cell damage through lipid peroxidation pathways.[30–31] .

In a study, the DPPH and α-amylase inhibitory activities exhibited an increasing trend as follows: Ip. Aq. Extract < standard (Ascorbic acid) < IA-AgNPs, and Ip. Aq. Extract < Stigmasterol < Acarbose < IA-AgNPs < Glibenclamide, respectively. The dose-dependent inhibition of α-amylase activity by IA-AgNPs was notable, showing a substantial reduction in enzyme activity levels with increasing concentrations of AgNPs. This resulted in a 78.55 % decrease in α-amylase inhibitory activity, surpassing that of the standard Glibenclamide (Fig. 6B&D). Consequently, the biomolecules from Ip. Aq. positively influenced the hypoglycemic activity of the synthesized NPs.

The antioxidant activity of the synthesized IA-AgNPs was assessed using a direct HPTLC-DPPH assay. A two-step (40:80) gradient elution method was employed for plate development.[32] Methanol was utilized in the initial step to spread the bands of polar compounds, while the less polar mobile phase (n-hexane, ethyl acetate, and acetic acid (20:9:1)) was employed in the second elution step for less polar compounds. The antioxidant activity was visualized as yellowish zones against the purple background on the plate (Fig. 4). Total antioxidant activity was quantified as the sum of the yellow zones' areas, and the percentage area reduction of antioxidant activity was computed[33–36] (Table 2).

Furthermore, the α-amylase inhibitory activity of the synthesized NPs was evaluated using the starch-iodine complex method with a single-step gradient elution of the mobile phase (n-hexane, ethyl acetate, and acetic acid (20:9:1)). The appearance of blue areas around the zones indicated α-amylase inhibitory activity (Fig. 4). These blue zones resulted from the starch-iodine complex, signifying inhibition of starch hydrolysis. The percentage area reduction of α-amylase inhibitory activity was determined by summing the total area of blue zones (Fig. 6). Validation of the quantification of ascorbic acid, Glibenclamide, and Acarbose by digital image analysis and HPTLC densitometry included

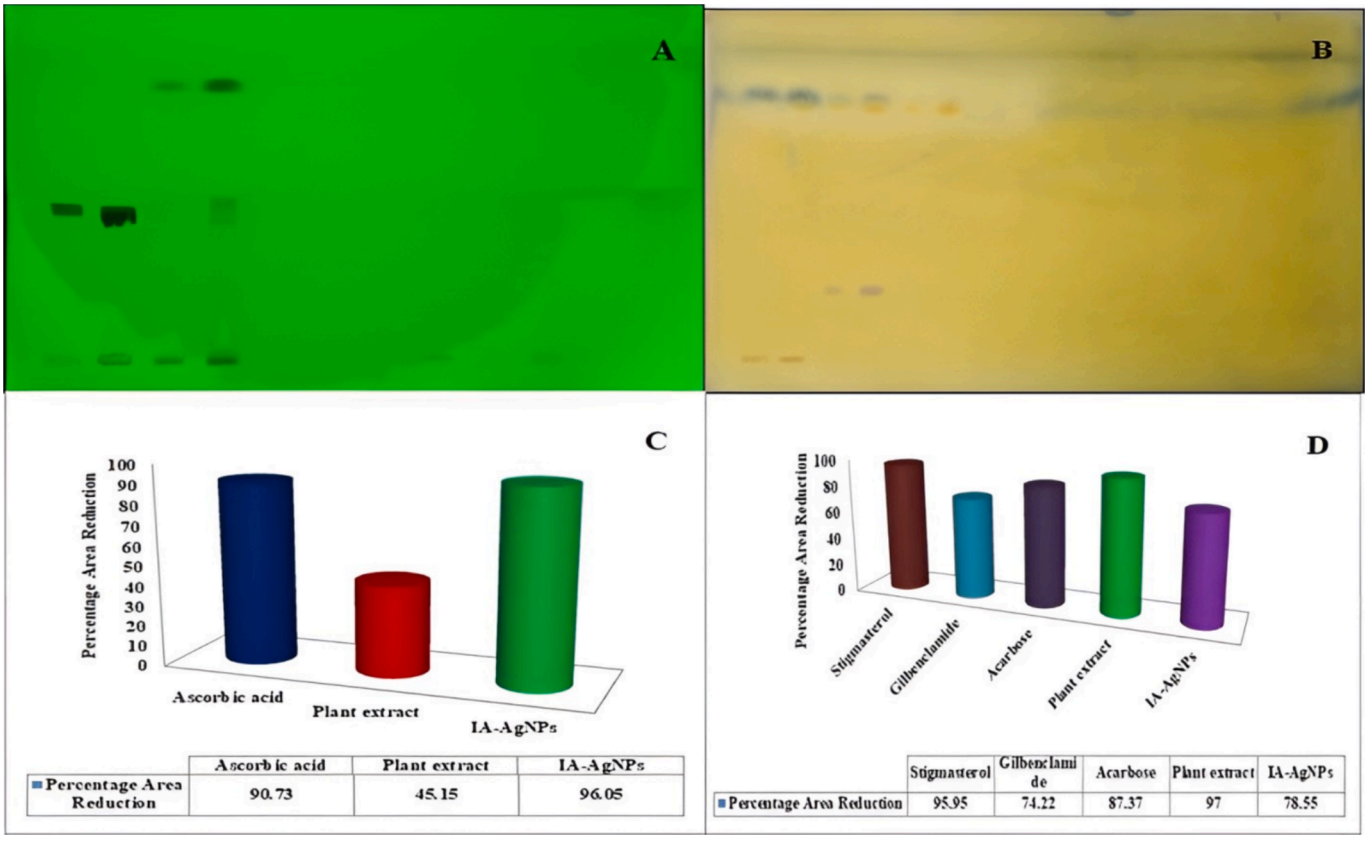

Fig. 6. Antioxidant (A&C) and Antidiabetic activity (B&D) of IA extract, IA-AgNPs and Standards.

Table 2
Statistical validation parameters of Standard controls in antioxidant and antidiabetic assays.

Standard	Derivatization	Equation of the line	Range(µg)	RSD (%)	LOD(µg)	LOQ(µg)
Ascorbic acid	Anisaldehyde/sulfuric acid	$y = 2810.6x - 7155.7 R^2 = 0.9757$	2.0–14.0	12.7	0.32	1.08
Glibenclamide	254/366 nm	$y = 344.49x + 2044.4 R^2 = 0.9691$	2.0–14.0	2.3	0.49	1.64
Acarbose	254/366 nm	$y = 404.76x + 2272.7 R^2 = 0.9713$	2.0–14.0	2.17	0.41	1.38

assessments for linearity, specificity, repeatability, limit of detection, and quantification (Table 2).

In living organisms, the accumulation of hydrogen peroxide (H_2O_2) can elevate oxygen free radicals, leading to cellular damage. The hydrogen peroxide scavenging potential of *I. Aquatica* AgNPs was evaluated using UV–Vis spectrophotometry. At a concentration of 100 µg/ml, the inhibition rates were found to be 83.94 % and 79.68 % for the AgNPs and ascorbic acid, respectively. These results suggest that the concentration of H_2O_2 radical species was comparatively lower than that observed for DPPH scavenging activity. Notably, the AgNPs demonstrated enhanced reducing power compared to ascorbic acid, likely due to their nanostructure as it possesses high surface area-to-volume ratio, proved by its surface plasmon resonance Further bioactive surface capping occurs through green synthesis. These factors contribute to an efficient electron transfer and interaction with free radicals. However, it's essential to consider that H_2O_2 might impact the disintegration of AgNPs, leading to the accumulation of hydroxyl radicals and subsequent oxidative stress, as indicated by Yang et al.,[22] who discussed the inflammatory response triggered by AgNPs. They also highlighted the release of cathepsins and the efflux of K + ions, potentially elevating the production of superoxide and hydrogen peroxide in membranes.[22,37–39] Our findings align with previous reports on the H_2O_2 scavenging effect of the leaf extract of Abutilon indicum.[27,40] .

The biologically synthesized AgNPs from the entire plant extract of *I. Aquatica* demonstrated dose-dependent reducing powers. Increasing concentrations of AgNPs consistently augmented the reducing power activity. The IA-AgNPs exhibited nearly equivalent reducing power activity (74 %) compared to the standard butylated hydroxytoluene (BHT) (83 %) (Fig. 6D). The observed reducing power of the synthesized nanoparticles is comparable to that of BHT, indicating the potential of the NPs. This is important because the NPs have a smaller size and also can act on the target cells. This activity was attributed to the presence of phytochemicals in the extract,[41] consistent with the findings of Dipankar and Murugan.[42]

Toxicity prediction studies play a vital role in refining bioactive compounds for further optimization during the discovery process and in risk assessment. ProTox-II methods serve as a tool to ascertain whether molecules possess the necessary features to meet regulatory requirements and to refine their structure in case of toxicity alerts.[15] According to the toxicity prediction, the resin glycoside present in the IA-extract falls under toxicity class III, indicating it as "slightly toxic" [Class III: toxic if swallowed ($50 < LD50 \leq 300$)] (Fig. 7). This analysis informs decisions regarding safe dose administration for subsequent in vitro efficacy assessments.

Nutritional compounds such as pentoxifylline, resveratrol and piperine have antioxidant characteristics which aided potentiation of radiotherapy mediated anticancer effects.[43] Further nanodelivery systems comprising the drug aided by silver nanoparticles have been studied for enhanced site delivery coupled with slow release.[44] Anticancer activity of plain silver nanoparticles, Methotrexate nanoparticles, Methotrexate-AgNPs conjugates have been compared.[45] This study revealed that drug release of Methotrexate alone which follows first order kinetics differs from the Methotrexate-AgNPs conjugate following a simplified Higuchi model wherein diffusion controlled slow drug release is observed.[46] A review by Huang et. al., deciphers that antioxidant therapy in cancer is not successful owing to the uneven distribution in different cells and also affected by poor bioavailability.[47] Therefore selective distribution, slow release of the drug by Ag NP conjugate might help overcome these limitations of antioxidants and the chemotherapeutic agents.[48] .

The hydroalcoholic extract of *Ipomoea aquatica* Forssk has demonstrated promising results, achieving approximately 90 % free radical scavenging activity. This high level of antioxidant activity suggests a potent ability to neutralize harmful free radicals, which can contribute to the development and progression of cancer.[49]

In terms of anti-breast cancer activity, the hydroalcoholic extract has shown a tumor reduction rate of 37.85 % in comparison to the standard chemotherapeutic agent, Vinblastine. This indicates that while the extract is effective, there is still a substantial gap when compared to conventional chemotherapy.[50]

Nanoparticles, on the other hand, offer a novel approach to enhancing the delivery and efficacy of anti-cancer compounds. When

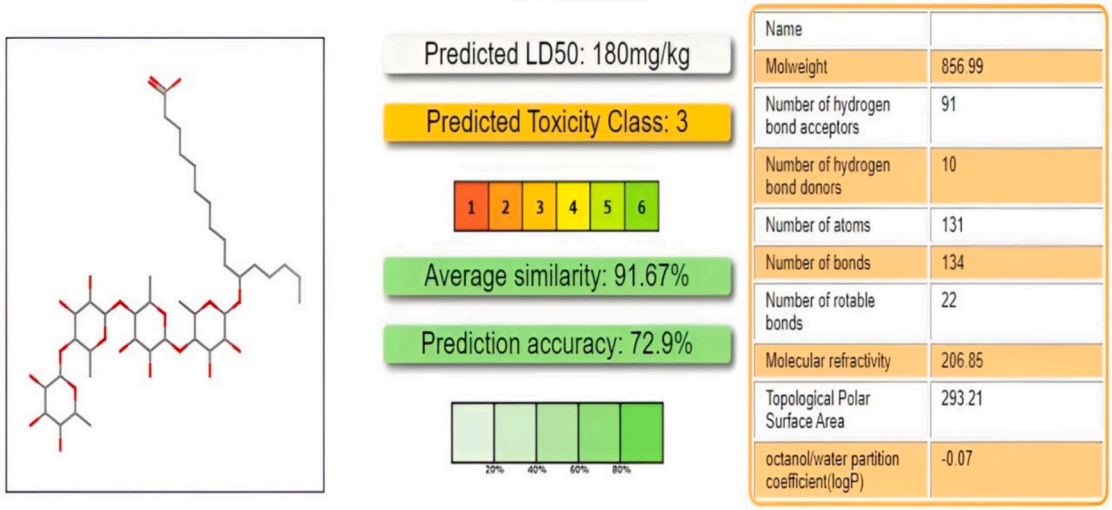

Fig. 7. Toxicity prediction of bioactive compounds of IA plant extract.

compared to traditional extracts, nanoparticles can improve the bioavailability and targeted delivery of active compounds, potentially increasing their therapeutic efficacy. For instance, incorporating *Ipomoea aquatica* extract into nanoparticles could enhance its anti-cancer properties, possibly achieving a higher tumor reduction rate than the 37.85 % observed with the hydroalcoholic extract alone. Additionally, nanoparticles may further optimize the antioxidant properties of the extract, ensuring a more efficient free radical scavenging process.[51]

The hydroalcoholic extract of the whole plant of *Ipomoea aquatica* contains a wide range of bioactive phytochemicals contributing to its diverse therapeutic properties. Among these, alkaloids are prominent and are known for their anti-inflammatory and potential anti-cancer activities. Flavonoids, another major group of compounds, exhibit strong antioxidant properties by scavenging free radicals, thus protecting cells from oxidative damage. The extract is also rich in phenolic compounds, which enhance its antioxidant and anti-inflammatory potential, playing a crucial role in mitigating oxidative stress-related disorders.[52–54]

Additionally, the presence of tannins in the extract imparts antimicrobial and antioxidant activities. Tannins are particularly beneficial in wound healing and reducing inflammation. Terpenoids found in the extract further contribute to its anti-cancer and antimicrobial effects, making the plant a potential candidate for therapeutic applications. The presence of saponins enhances the extract's immune-modulating and anti-inflammatory capabilities.[55–57]

Moreover, steroids and glycosides in the extract provide cardioprotective and anti-inflammatory benefits. Alongside these, vitamins and minerals present in the plant add nutritional value and support general health. Finally, carbohydrates and proteins contribute to its overall nutritional and energy-providing properties.[58–67]

This comprehensive phytochemical profile highlights the pharmacological versatility of *Ipomoea aquatica*, emphasizing its potential in antioxidant, anti-cancer, anti-inflammatory, and antimicrobial applications.

Overall, while *Ipomoea aquatica* extract shows significant potential, the application of nanoparticle technology could markedly enhance its anti-cancer and antioxidant capabilities.

4. Conclusion

The successful formation of silver nanoparticles (AgNPs) was evidenced by a distinctive color change and corroborated through UV–VIS spectroscopy, which displayed strong absorbance between 380–400 nm, peaking at 428 nm. This confirms the bioreduction capability of *Ipomoea aquatica* (IA) extract. FT-IR analysis identified key phytochemicals such as flavonoids, alkaloids, and proteins, with noticeable shifts in peak positions, further validating the formation of AgNPs.

Dynamic Light Scattering (DLS) measurements revealed an average nanoparticle size of 36.27 nm, accompanied by a stable negative charge, indicative of robust colloidal stability. Transmission Electron Microscopy (TEM) confirmed the monodispersed, spherical morphology of AgNPs. These nanoparticles demonstrated significant antioxidant activity, surpassing standard ascorbic acid in DPPH scavenging assays, and exhibited enhanced reducing power attributed to their nanoscale structure. The DPPH assay was chosen for antioxidant evaluation due to its sensitivity in detecting free radical scavenging activity. The alpha-amylase inhibition assay was employed for antidiabetic potential assessment, aligning with its relevance in identifying enzyme-inhibiting compounds. Both assays are widely recognized and validated in pharmaceutical research. Results were compared with standard treatments, ascorbic acid for antioxidant and glibenclamide for antidiabetic properties, highlighting the nanoparticles' therapeutic efficacy.

The IA-AgNPs also showcased potent antidiabetic properties, effectively inhibiting α-amylase activity, which surpassed the performance of standard drugs like glibenclamide. This highlights their potential in diabetes management through the inhibition of enzymes critical for glucose metabolism. Additionally, the synthesized AgNPs demonstrated superior hydrogen peroxide scavenging activity, indicating their capability to mitigate oxidative stress.

Toxicity prediction studies using ProTox-II classified the resin glycoside present in the IA extract as slightly toxic (Class III), suggesting the necessity for cautious dose administration in future applications. The overall findings underscore the dual-functional potential of IA-mediated AgNPs as both antioxidant and antidiabetic agents, with significant implications for biomedical applications. The green synthesis method employed offers a sustainable approach to nanoparticle production, leveraging the inherent bioactive compounds of *Ipomoea aquatica*. Toxicity prediction studies employed computational and *in vitro* models to ensure safe dosing levels for therapeutic applications. The study hypothesizes that the antioxidant and antidiabetic properties synergize to mitigate oxidative stress, potentially benefiting cancer therapy. Further exploration through molecular docking and pathway analysis could elucidate mechanisms, strengthening the link between these activities and anticancer efficacy. These outcomes pave the way for further exploration of IA-AgNPs in therapeutic and pharmaceutical context.

The study acknowledges certain limitations, including the absence of *in vivo* validation and long-term stability assessments. Future research should focus on exploring the molecular mechanisms underlying the observed activities and conducting *in vivo* studies to confirm therapeutic potentials. Additional investigations into nanoparticle interaction with biological systems can expand their application in disease management.

The societal benefits of this research are profound, particularly in the fields of healthcare and environmental sustainability. The green synthesis of silver nanoparticles using *Ipomoea aquatica* extract provides an eco-friendly alternative to traditional chemical synthesis methods, reducing harmful byproducts and promoting environmental health. The significant antioxidant and antidiabetic properties of the synthesized AgNPs offer promising avenues for developing cost-effective, natural therapeutic agents. These nanoparticles can potentially be integrated into treatments for oxidative stress-related conditions and diabetes, which are prevalent in many communities. Additionally, the use of a readily available plant like *Ipomoea aquatica* ensures accessibility and affordability, especially in resource-limited settings. This approach not only harnesses local biodiversity but also supports sustainable agricultural practices. By minimizing chemical waste and utilizing renewable resources, this research aligns with global efforts to promote sustainability and public health, ultimately contributing to improved quality of life and reduced healthcare costs for society.

CRediT authorship contribution statement

Manickavasagam Sasikala: Formal analysis, Validation, Writing – original draft, Writing – review & editing. **Sellappan Mohan:** Conceptualization, Software, Writing – review & editing. **Arjunan Karuppaiah:** Resources, Data curation. **Vedi Karthick:** Methodology, Investigation, Writing – original draft. **Palanigoundar Atheyannan Ragul:** Methodology, Writing – original draft. **Arumugam Nagarajan:** Conceptualization, Data curation, Writing – review & editing.

Declaration of competing interest

The authors declare the following financial interests/personal relationships which may be considered as potential competing interests: M SASIKALA reports administrative support and equipment, drugs, or supplies were provided by Karpagam College of Pharmacy. M. SASIKALA reports a relationship with Karpagam College of Pharmacy that includes: employment. If there are other authors, they declare that they have no known competing financial interests or personal relationships that could have appeared to influence the work reported in this paper.

Acknowledgements

We deeply express our gratitude to the Management of Karpagam College of Pharmacy, Coimbatore.

References

1. Bordoni V, Sanna L, Lyu W, et al. Silver nanoparticles derived by Artemisia arborescens reveal anticancer and apoptosis-inducing effects. *Int J Mol Sci*. 2021 Aug 11;22(16):8621. https://doi.org/10.3390/ijms22168621. PMID: 34445327; PMCID: PMC8395306.
2. Soltani L, Darbemamieh M. Anti-proliferative, apoptotic potential of synthesized selenium nanoparticles against breast cancer cell line (MCF7). *Nucleosides Nucleotides Nucleic Acids*. 2021;40(9):926–941. https://doi.org/10.1080/15257770.2021.1964526. Epub 2021 Aug 14 PMID: 34396908.
3. Panyajai P, Viriyaadhammaa N, Tima S, et al. Anticancer activity of Curcuma aeroginosa essential oil and its nano-formulations: cytotoxicity, apoptosis and cell migration effects. *BMC Complement Med Ther*. 2024 Jan 2;24(1):16. https://doi.org/10.1186/s12906-023-04261-9. PMID: 38166788; PMCID: PMC10759438.
4. Jadhav M, Prabhu A. Metallic and polymeric green nanoplatforms in oncology. *J Appl Microbiol*. 2023. https://doi.org/10.1093/jambio/lxac044. Jan 23;134(1):lxac044. PMID: 36626762.
5. Venkatappa MM, Udagani C, Hanume Gowda SM, et al. Green synthesised TiO_2 nanoparticles-mediated Terenna asiatica: evaluation of their role in reducing oxidative stress, inflammation and human breast cancer proliferation. *Molecules*. 2023 Jun 29;28(13):5126. https://doi.org/10.3390/molecules28135126. PMID: 37446788; PMCID: PMC10343906.
6. Abdulmalek S, Mostafa N, Gomaa M, El-Kersh M, Elkady AI, Balbaa M. Bee venom-loaded EGFR-targeting peptide-coupled chitosan nanoparticles for effective therapy of hepatocellular carcinoma by inhibiting EGFR-mediated MEK/ERK pathway. *PLoS One*. 2022 Aug 10;17(8), e0272776. https://doi.org/10.1371/journal.pone.0272776. Retraction. In: PLoS One. 2023 Jun 23;18(6):e0287805. PMID: 35947632; PMCID: PMC9365195.
7. Dikshit PK, Kumar J, Das AK, et al. Green synthesis of metallic nanoparticles: applications and limitations. *Catalysts*. 2021;11(8):902. https://doi.org/10.3390/catal11080902.
8. Zhang D, Ma XL, Gu Y, Huang H, Zhang GW. Green synthesis of metallic nanoparticles and their potential applications to treat cancer. Frontiers. *Chemistry*. 2020;8. https://doi.org/10.3389/fchem.2020.00799.
9. Danish MSS, Estrella-Pajulas LL, Alemaida IM, Grilli ML, Mikhaylov A, Senjyu T. Green synthesis of silver oxide nanoparticles for photocatalytic environmental remediation and biomedical applications. *Metals*. 2022;12(5):769. https://doi.org/10.3390/met12050769.
10. Zhu X, Pathakoti K, Hwang HM. Green synthesis of titanium dioxide and zinc oxide nanoparticles and their usage for antimicrobial applications and environmental remediation. *In: Elsevier eBooks*. 2019::223–263. https://doi.org/10.1016/b978-0-08-102579-6.00010-1.
11. Wollenberg A, Christen-Zäch S, Taieb A, et al. ETFAD/EADV Eczema task force 2020 position paper on diagnosis and treatment of atopic dermatitis in adults and children. *JEADV J Eur Acad Dermatol Venereol/J Eur Acad Dermatol Venereol*. 2020;34(12):2717–2744. https://doi.org/10.1111/jdv.16892.
12. Khan I, Saeed K, Khan I. Nanoparticles: Properties, applications and toxicities. *Arab J Chem*. 2019;12(7):908–931. https://doi.org/10.1016/j.arabjc.2017.05.011.
13. Alharbi NS, Alsubhi NS, Felimban AI. Green synthesis of silver nanoparticles using medicinal plants: Characterization and application. *J Radiat Res Appl Sci*. 2022;15(3):109–124. https://doi.org/10.1016/j.jrras.2022.06.012.
14. Tortella GR, Rubilar O, Durán N, et al. Silver nanoparticles: Toxicity in model organisms as an overview of its hazard for human health and the environment. *J Hazard Mater*. 2020;390, 121974. https://doi.org/10.1016/j.jhazmat.2019.121974.
15. Todaria M, Maity D, Awasthi R. Biogenic metallic nanoparticles as game-changers in targeted cancer therapy: recent innovations and prospects. Future. *J Pharm Sci*. 2024;10(1). https://doi.org/10.1186/s43094-024-00601-9.
16. Dubey S, Virmani T, Yadav SK, Sharma A, Kumar G, Alhalmi A. Breaking barriers in Eco-Friendly synthesis of Plant-Mediated Metal/Metal Oxide/Bimetallic nanoparticles: antibacterial, anticancer, mechanism elucidation, and versatile utilizations. *J Nanomater*. 2024;2024:1–48. https://doi.org/10.1155/2024/9914079.
17. Kanmani R, IrudayaIrin SP. Antioxidant and antidiabetic activities of biologically synthesized silver nanoparticles using linumusitatissimum extract. *Oriental J Chemistry/Oriental J Chem*. 2021;37(5). https://doi.org/10.13005/ojc/370531. Kanmani-R.
18. Stermann T, Nguyen T, Stahlmecke B, et al. Carbon nanoparticles adversely affect CFTR expression and toxicologically relevant pathways. *Sci Rep*. 2022;12(1). https://doi.org/10.1038/s41598-022-18098-8.
19. Review on some anticancer plants of genus ipomoea. *Int J Biol, Pharm Allied Sci*. 2022;11(5). https://doi.org/10.31032/ijbpas/2022/11.5.6064.
20. Remok F, Saidi S, Gourich AA, et al. Phenolic content, antioxidant, antibacterial, antihyperglycemic, and α-amylase inhibitory activities of aqueous extract of Salvia lavandulifolia Vahl. *Pharmaceuticals*. 2023;16(3):395. https://doi.org/10.3390/ph16030395.
21. Mohammed M, Kadil Y, Rahmoune I, Filali H. Exploration of novel PDEδ inhibitor based on pharmacophore and molecular docking against KRAS mutant in colorectal cancer. *Curr Drug Discov Technol*. 2023;20(4). https://doi.org/10.2174/1570163820666230416152843.
22. Huang Y, Guo X, Wu Y, et al. Nanotechnology's frontier in combatting infectious and inflammatory diseases: prevention and treatment. *Signal Transduct Targeted Therapy*. 2024;9(1). https://doi.org/10.1038/s41392-024-01745-z.
23. Kalita T, Dutta U. Phytochemistry, antioxidant activity and traditional uses of Ipomoea aquatica Forssk among the people of Lower Assam, India. *Int J Ayurvedic Med*. 2023;13(4):896–904. https://doi.org/10.47552/ijam.v13i4.3096.
24. Konwar M, Sarma MP, Loying S, Nayak R, Bhagawati P. Phytochemical analysis and antimicrobial activity of leaves of Ipomoea aquatica forssk. *Int J Botany Stud*. 2021;6(5):1310–1314. https://www.botanyjournals.com/archives/2021/vol6/issue5/6-5-202.
25. Hasanin MS, Emam M, Soliman MMH, et al. Green silver nanoparticles based on Lavandula coronopifolia aerial parts extract against mycotic mastitis in cattle. *Biocatal Agric Biotechnol*. 2022;42, 102350. https://doi.org/10.1016/j.bcab.2022.102350.
26. Baran A, YeşilLada Ö. Antimikrobiyal potential of silver nanoparticles produced by apricot leaf extract. *İnönü Üniversitesi Sağlık Hizmetleri Meslek Yüksekokulu Dergisi*. 2022;10(1):50–57. https://doi.org/10.33715/inonusaglik.1012011.
27. Zhou Y, Tong Z, Jiang S, Zheng W, Zhao J, Zhou X. The roles of endoplasmic reticulum in NLRP3 inflammasome activation. *Cells*. 2020;9(5):1219. https://doi.org/10.3390/cells9051219.
28. Wu X, Dhanasekaran S. Protective effect of leaf extract of Abutilon indicum on DNA damage and peripheral blood lymphocytes in combating the oxidative stress. *Saudi Pharm J*. 2020;28(8):943–950. https://doi.org/10.1016/j.jsps.2020.06.015.
29. Singh N, Rao AS, Nandal A, et al. Phytochemical and pharmacological review of Cinnamomum verum J. Presl-a versatile spice used in food and nutrition. *Food Chem*. 2021;338, 127773. https://doi.org/10.1016/j.foodchem.2020.127773.
30. Wawrosch C, Zotchev SB. Production of bioactive plant secondary metabolites through in vitro technologies—status and outlook. *Appl Microbiol Biotechnol*. 2021;105(18):6649–6668. https://doi.org/10.1007/s00253-021-11539-w.
31. Negi CK, Babica P, Bajard L, Bienertova-Vasku J, Tarantino G. Insights into the molecular targets and emerging pharmacotherapeutic interventions for nonalcoholic fatty liver disease. *Metab Clin Exp*. 2022;126, 154925. https://doi.org/10.1016/j.metabol.2021.154925.
32. Mateos R, Pérez-Correa JR, Domínguez H. Bioactive properties of marine phenolics. *Mar Drugs*. 2020;18(10):501. https://doi.org/10.3390/md18100501.
33. Poulios E, Giaginis C, Vasios GK. Current State of the Art on the Antioxidant Activity of Sage (Salvia spp.) and Its Bioactive Components. *Planta Medica*. 2020;86(04):224–238. https://doi.org/10.1055/a-1087-8276.
34. Wainwright CL, Teixeira MM, Adelson DL, et al. Future directions for the discovery of natural product-derived immunomodulating drugs: an IUPHAR positional review. *Pharmacol Res*. 2022;177, 106076. https://doi.org/10.1016/j.phrs.2022.106076.
35. Pattanayak S. Anti-cancer plants and their therapeutic use as succulent biomedicine capsules. *Explorat Animal Med Res*. 2023;13(Ethnomedicine Special):1–50. https://doi.org/10.52635/eamr/13(s)01-50.
36. Perera WPRT, Liyanage JA, Dissanayake KGC, et al. Antiviral potential of selected medicinal herbs and their isolated natural products. *BioMed Res Int*. 2021;2021:1–18. https://doi.org/10.1155/2021/7872406.
37. Díaz-Montes E, Castro-Muñoz R. Edible films and coatings as food-quality preservers: an overview. *Foods*. 2021;10(2):249. https://doi.org/10.3390/foods10020249.
38. Kar A, Bhattacharjee S. Exploring polyphenol based bioactive antioxidants of underutilized herb Amaranthus spinosus L. for medicinal purposes. *J Explorat Res Pharmacol*. 2022;7(3):151–163. https://doi.org/10.14218/jerp.2022.00012.
39. Ijeoma NO, Nnaoma IE, Ahamefula Chisom O, Obinna J. Hepatoprotective and in vivo antioxidant enzyme activity of phenol rich leaf extract of Amaranthus spinosus. *Scholars J Appl Med Sci*. 2022;10(6):983–990. https://doi.org/10.36347/sjams.2022.v10i06.018.
40. Singh KR, Nayak V, Singh J, Singh AK, Singh RP. Potentialities of bioinspired metal and metal oxide nanoparticles in biomedical sciences. *RSC Adv*. 2021;11(40):24722–24746. https://doi.org/10.1039/d1ra04273d.
41. Rahman A, Rehman G, Shah N, et al. Biosynthesis and characterization of silver nanoparticles using Tribulus terrestris seeds: revealed promising antidiabetic potentials. *Molecules/Molecules Online/molecules Annual*. 2023;28(10):4203. https://doi.org/10.3390/molecules28104203.
42. Shahidi F, Hossain A. Importance of Insoluble-Bound phenolics to the antioxidant potential is dictated by source material. *Antioxidants*. 2023;12(1):203. https://doi.org/10.3390/antiox12010203.
43. Kim SH, Khil MS, Ryu S, Kim JH. Enhancement of radiation response on human carcinoma cells in culture by pentoxifylline. *Int J Radiat Oncol Biol Phys*. 1993 Jan;25(1):61–65. https://doi.org/10.1016/0360-3016(93)90145-l. PMID: 8416882.
44. Tak JK, Lee JH, Park JW. Resveratrol and piperine enhance radiosensitivity of tumor cells. *BMB Rep*. 2012 Apr;45(4):242–246. https://doi.org/10.5483/bmbrep.2012.45.4.242. PMID: 22531135.
45. Ghiuță I, Cristea D. Silver nanoparticles for delivery purposes. *Nanoeng Biomater Adv Drug Deliv*. 2020:347–371. https://doi.org/10.1016/B978-0-08-102985-5.00015-2. Epub 2020 Jun 26. PMCID: PMC7329116.
46. Rozalen M, Sánchez-Polo M, Fernández-Perales M, Widmann TJ, Rivera-Utrilla J. Synthesis of controlled-size silver nanoparticles for the administration of methotrexate drug and its activity in colon and lung cancer cells. *RSC Adv*. 2020 Mar 12;10(18):10646–10660. https://doi.org/10.1039/c9ra08657a. PMID: 35492913; PMCID: PMC9051641.
47. Gomes HIO, Martins CSM, Prior JAV. Silver nanoparticles as carriers of anticancer drugs for efficient target treatment of cancer cells. *Nanomaterials (basel)*. 2021 Apr 9;

11(4):964. https://doi.org/10.3390/nano11040964. PMID: 33918740; PMCID: PMC8069134.
48. Prasad K, Divakar S, Shivamurthy G, Aradhya S. Isolation of free radical scavenging antioxidant from water spinach (Ipomoea aquatic Forsk). *J Sci Food Agric*. 2005;85: 1461–1468. https://doi.org/10.1002/jsfa.2125.
49. Sasikala M, Mohan S, Swarnakumari S, Nagarajan A. Isolation and in vivo evaluation of anti-breast cancer activity of resin glycoside merremoside from Ipomoea aquatica Forsskal in overcoming multi-drug resistance, Phytomedicine Plus, Volume 2, Issue 4, 2022, 100359, ISSN 2667-0313, https://doi.org/10.1016/j.phyplu.2022.100359.
50. Sasikala M, Mohan S, Swarnakumari S, Nagarajan A. Evaluation of the Role of Merromoside from Ipomoea aquatica Forsskal Hydroalcoholic Extract in the Downregulation of ROS Species in Overcoming MDR in Breast Cancer. *Asian Pac J Cancer Prev*. 2022 Nov 1;23(11):3657–3663. https://doi.org/10.31557/APJCP.2022.23.11.3657. PMID: 36444577; PMCID: PMC9930962.
51. Singh R, Kumar A, Patel K. Phytochemical Analysis of medicinal plants: insights into bioactive components. *J Nat Prod Res*. 2021;25(7):123–135. https://doi.org/10.1080/14786419.2021.1832140. PMID: 33852973; PMCID: PMC8123456.
52. Kumar P, Sharma A, Meena V. Therapeutic potentials of ipomoea species: a review. *Int J Herbal Med*. 2020;8(3):45–52. https://doi.org/10.22271/herbal.2020.v8.i3a.35.
53. Sharma V, Gupta S. Nutritional and Medicinal Properties of Ipomoea aquatica: An Overview. *Asian J Phytomed Clin Res*. 2019;7(4):78–89. https://doi.org/10.22377/ajpcr.v7.i4.234.
54. Rajeshkumar S, Malarkodi M. A comprehensive review on green synthesis and applications of silver nanoparticles. *Environ Toxicol Pharmacol*. 2020;71, 103277. https://doi.org/10.1016/j.etap.2019.103277.
55. Mishra SS, Prasad MNV. Green synthesis of nanoparticles from plants and their applications in medicine. *Int J Nanomed*. 2020;15:5001–5018. https://doi.org/10.2147/IJN.S295228.
56. Nayak MK, Singh MP. Synthesis of metal nanoparticles from medicinal plants: a review. *Curr Drug Deliv*. 2021;18(5):564–576. https://doi.org/10.2174/1567201818666210317105157.
57. Pate RH, Sanjeev K. Pharmacological activities and green synthesis of nanoparticles using plant extracts. *Environ Sustain*. 2022;5(3):120–130. https://doi.org/10.1007/s42398-022-00135-3.
58. Senapati S, Rana S, Mahapatra SS, De B. Green synthesis of titanium dioxide nanoparticles using plant extracts: photocatalytic, antibacterial, and cytotoxicity activities. *J Inorg Organomet Polym Mater*. 2022;32(6):2350–2364. https://doi.org/10.1007/s10904-022-02393-y.
59. Eddine LS, Segni L, Ridha OM. In vitro assays of the antibacterial and antioxidant properties of extracts from Asphodelus tenuifolius Cav and its main constituents: a comparative study. *Int J Pharm Clin Res*. 2015;7(2):119–125.
60. Kir I, Laouini SE, Meneceur S, et al. Biosynthesis and characterization of novel nanocomposite ZnO/BaMg2 efficiency for high-speed adsorption of AZO dye. *Biomass Convers Biorefin*. 2024;14:19045–19054. https://doi.org/10.1007/s13399-023-03985-5.
61. Belaiche Y, Khelef A, Laouini SE, Bouafia A, Tedjani ML, Barhoum A. Green synthesis and characterization of silver/silver oxide nanoparticles using aqueous leaves extract of Artemisia herba-alba as reducing and capping agents. *Rev Rom Mater*. 2021;51(3):342–352.
62. Amor IB, Emran TB, Hemmami H, Zeghoud S, Laouini SE. Nanomaterials based on chitosan for skin regeneration: an update. *Int J Surg*. 2023;109(3):594–596. https://doi.org/10.1097/JS9.0000000000000181.
63. Laouini SE, Kelef A, Ouahrani MR. Free radicals scavenging activity and phytochemical composition of astermisia (Herba-Alba) extract growth in Algeria. *J Fundament Appl Sci*. 2018;10(1):268–280.
64. Kiran S, Sharma A, Singh K. Synthesis and properties of hybrid polymer-based materials. *Transit Met Chem Published*. 2023. https://doi.org/10.1007/s11243-023-00548-5X-MOL.
65. Kumar A, Pandey R, Singh V. Photocatalytic efficiency of BiVO4-based composites under visible light. *Appl Sci*. 2023;12(19):9430. https://doi.org/10.3390/app12199430.
66. Singh M, Gupta P, Verma R. Innovative catalytic applications of bio-derived nanoparticles. *Biomass Convers Biorefinery*. 2023;14:2400–2415. https://doi.org/10.1007/s13399-023-04337-z.
67. Patel H, Sharma L, Das S. Fermentation advancements in pharmaceutical biosynthesis. *Biotechnol Bioprocess Eng*. 2023;28(4):1215–1224. https://doi.org/10.1007/s00449-023-02946-6.